ACS Partner Journal
ACCOUNTS of materials research



pubs.acs.org/amrcda
Article

# Heterogeneous Integration of Diamond

Oliver A. Williams,*,‡ Soumen Mandal,*,‡ and Jerome A. Cuenca*,‡

Cite This: https://doi.org/10.1021/accountsmr.4c00126



**CONSPECTUS:** The heterogeneous integration of materials offers new paradigms in many extreme applications, where single materials cannot solve the problem alone. Diamond has a plethora of superlative properties that make it attractive in a diverse array of applications, such as its unique combination of unrivalled thermal conductivity combined with high electrical impedance; single photon emission at room temperature; superlative acoustic wave velocity, and Debye temperature. Most of these properties are directly related to diamond's atomically dense lattice of light carbon atoms, which has consequences such as difficulty in doping diamond n-type and low thermal coefficient of thermal expansion. This last property presents a significant problem for the growth of diamond on nondiamond materials as the linear coefficients of thermal expansion of other materials are often several times larger than diamond.

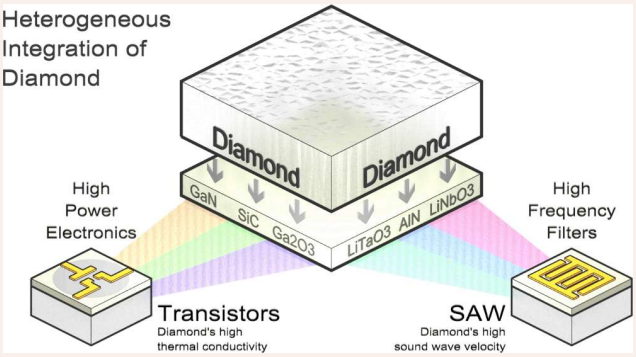


The integration of diamond with other materials is thus a complex and multifaceted problem, with various solutions with individual pros and cons. Our work focused on the growth of diamond directly on various materials or with enabling interlayers. In particular, we have focused on driving the self-assembly of diamond nanoparticles onto nondiamond surfaces as the precursors to diamond growth. This approach requires knowledge of the zeta potential as a function of pH of the surface to be treated as well as that of the diamond particles, and this Account provides a detailed summary of the most critical materials for diamond integration. The high density of nanodiamond particles as precursors for diamond growth is unfortunately not sufficient, and this Account discusses issues with adhesion and stress which are exacerbated by the aforementioned anomalously low thermal expansion coefficient.

In this Account, we review this approach with references to competing approaches, detailing unavoidable issues such as wafer bow, stresses, and the harsh environment of diamond chemical vapor deposition.

## 1. INTRODUCTION

The extreme properties of diamond are well documented (Table 1) and exploited in a wide range of applications from oil and gas drilling to quantum technologies. However, these properties can be a double-edged sword. For example, the atomic density of diamond yields unrivaled hardness, thermal conductivity, Debye temperature, and sound wave velocity. But this same property makes diamond difficult to dope efficiently, with 1% activation of its most successful dopant (boron) at room temperature.[1] N-type doping is even more problematic with activations energies greater than the bandgap of germanium (0.6 eV).[2] This doping limitation can be a significant advantage in quantum technologies, enabling the growth of very high purity materials with unrivalled coherence times.[3] The high Debye temperature of diamond helps room temperature single photon emission but can inhibit the transfer of heat across interfaces with other materials due to poor overlap of the phonon density of states.[4] The anomalously low coefficient of thermal expansion of diamond can be adventitious for optical components such as lenses and mirrors but is an Achilles' heel when integrating with other materials due to the high temperature of diamond growth.

The integration of diamond with other materials is the focus of this Account. Heterogeneous Integration promises a combination of synergistic properties of dissimilar materials for specific applications where no individual material suffices. There are several obvious combinations from Table 1 such as the thermal management of Si, GaN or $Ga_2O_3$ with diamond;[5,6] the combination of direct bandgap semiconductors such as GaN/GaAs etc with diamond for pumping of its single photon centers and the integration of diamond with piezoelectric materials for Micro-Electro-Mechanical Systems (MEMS) and acoustic devices.[7,8] These combinations circumvent diamond's poor performance as a semiconductor (a consequence of its high atomic density); its lack of efficient light emission (a consequence of its indirect bandgap), and its lack of piezo-

Received: April 23, 2024
Revised: July 31, 2024
Accepted: August 5, 2024

**Table 1. Diamond Material Properties Comparison**

| | Si | SiC | GaN | $Ga_2O_3$ | Diamond | Units |
|---|---|---|---|---|---|---|
| Bandgap | 1.1 | 2.2−3.3 | 3.4 | 4.8 | 5.5 | eV |
| Electron mobility | 1400 | 900 | 1500 | 200 | 2000 | $cm^2/(V\ s)$ |
| Hole mobility | 450 | 320 | 350 | N/A | 2000 | $cm^2/(V\ s)$ |
| Dielectric constant | 11.7 | 9.7 | 8.9 | 10.2 | 5.7 | - |
| Breakdown field | 0.3 | 3 | 5 | 3.8 | 10 | MV/cm |
| Thermal conductivity | 1.3 | 1.2 | 1.3 | 0.3 | 22 | W/cm·K |
| Debye temperature | 640 | 1200 | 600 | 800 | 2220 | K |
| CTE (300 K) | 2.5 | 4 | 3.2 | 1.8 | 1 | ppm/K |
| Acoustic velocity | 8000 | 12000 | 4400 | 3000−7000 | 20000 | m/s |
| Substrate Ø | 450 | 200 | 150 | 100 | 25 (300) | mm |

electricity (a consequence of its elemental and isotropic lattice) respectively. Superlative performance has been demonstrated with such combinations as GaN/diamond HEMTS and AlN/diamond Surface Acoustic Wave devices.[8]

There are several routes to the Heterogeneous Integration of diamond such as the growth of diamond on the foreign material, the growth of the foreign material on diamond, and wafer bonding the two materials. There are advantages and disadvantages of each approach. For the case of diamond growth on other materials, the main advantage is the ability to use single crystal materials of the foreign material if they can withstand the high temperatures and harsh environment of diamond growth. The process is also wafer scale as diamond reactors are commercially available with over 12 in. diameter capability. Critical disadvantages are the polycrystalline nature of the diamond and large wafer bow/stresses due to differences in the coefficients of thermal expansion.[9] Although diamond has been grown at temperatures down to 400 °C, the growth rate is not commercially viable for thicknesses beyond a few hundred nm and the quality degrades due to the nanocrystalline nature.[10] Thus, the growth of diamond on the foreign material can work well for thermal management of some materials such as GaN etc. but poorly for quantum applications due to the nature of the grown diamond. It is also attractive for devices such as MEMS or electrochemical electrodes, where bulk diamond is not necessary or even desirable. In the case of MEMS, the presence of a sacrificial underlayer is often essential, and diamond is not easily under etched.

For the growth of foreign material on diamond, lower temperatures may be possible depending on the material (for example, many piezoelectric materials can be sputtered at room temperature), leading to lower wafer bow and stress. Single crystal diamond could be used, which although is not quite wafer scale, sizes are increasing rapidly due to the synthetic gem market. The disadvantage is that few materials grow epitaxially on diamond; thus, it is the foreign material that is polycrystalline. This can work well for quantum technologies where the quality of the diamond is paramount, some photonic devices etc but the reduced quality of polycrystalline piezoelectrics can lead to undesirable insertion loss in Surface Acoustic Wave devices.[11]

Wafer bonding has recently shown promise in circumventing issues with both approaches above. There are multiple approaches including hydrophilic bonding, direct bonding, etc.[12−15] Surface Activated Wafer Bonding (SAWB) in particular provides a route to covalent bonds between potentially any materials with near atomically flat interfaces.[16] This is particularly important in the case of thermal management as heat transport through van der Waals bonded interfaces is limited.[17] In SAWB, wafers are irradiated with Ar ions under ultrahigh vacuum to remove surface contaminants and termination. When the wafers are brought into contact with one another, the dangling bonds created at their surfaces heal to form covalent bonds between the two materials. As this is a room temperature technique, it does not result in high wafer bow and avoids the harsh environment of diamond growth. This enables the combination of many new materials hitherto impossible, with the main downside being the requirement of atomically flat surfaces and very low surface particle contamination. Thus, the Chemical Mechanical Planarization of diamond is critical.[18,19] There is also a finite (∼1 nm) amorphous interlayer between the diamond and foreign material[20] which will have poor electrical properties and lead to states within the bandgap.

This Account focuses on the growth of diamond on nondiamond materials. For this approach to be successful, several conditions must be met. First, the material must be resistant to the harsh environment of diamond growth, both the growth temperature and also critically the dense atomic hydrogen plasma. In some cases, the in-diffusion of carbon species into the material may have negative consequences, such as for transistor channels. Second, the nucleation of diamond on the material must be possible, or an appropriate interlayer must be used to enable it. Third, the diamond must also adhere, preferably via a carbide bond, to withstand the thermal stresses generated by the mismatch in the coefficient of thermal expansion on cool down from chemical vapor deposition.

## 2. NUCLEATION/SEEDING

The growth of diamond on nondiamond substrates generally requires surface pretreatments due to a combination of the high surface energy of diamond, competition of nondiamond phases and the low sticking coefficient of the nucleation precursors. For an extensive review of the various approaches the reader is referred to a recent review,[21] for brevity here we focus on the most prevalent approach for initiating diamond growth on nondiamond substrates, namely the "seeding" with diamond particles. The term "nucleation" is not strictly speaking accurate in this context as the diamond particles act as "seeds" upon which diamond grows epitaxially. Early approaches involved mechanical abrasion with diamond grit or bombardment of surfaces with micrometer-sized particles via ultrasonic cavitation in colloids. It was later found that these methods leave diamond debris behind[22] and thus a logical evolution was to use the smallest diamonds available as seeds as this should lead to the highest nucleation density (by packing density). The smallest diamonds available (excepting the diamondoids which are volatile and poor nucleation sites[23]) are those formed by detonation of high explosives such as TNT and RDX, often termed "Detonation Nanodiamond (DND) or Ultra-Dispersed


https://doi.org/10.1021/accountsmr.4c00126
Acc. Mater. Res. XXXX, XXX, XXX−XXX

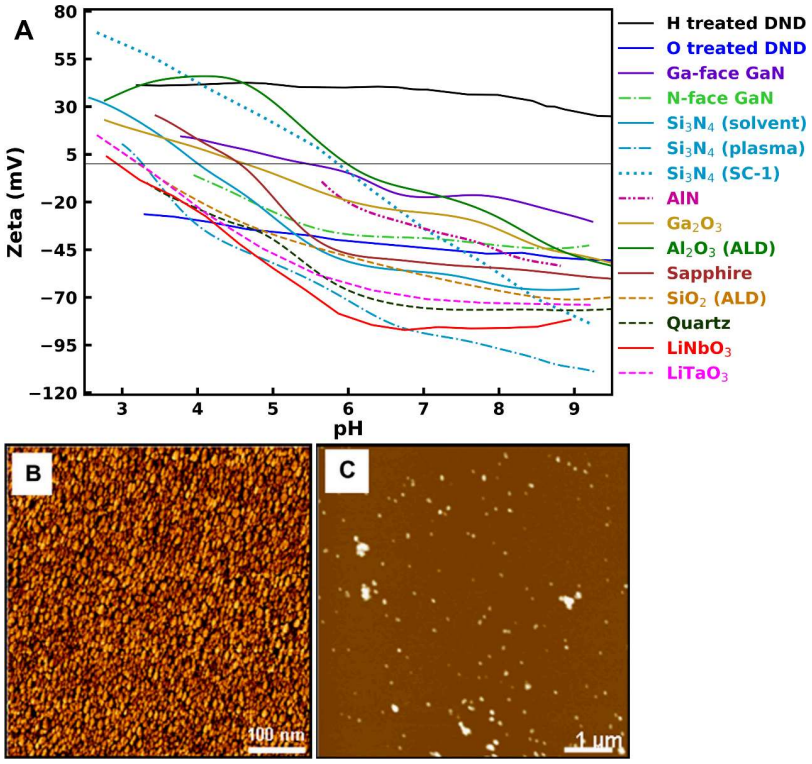


**Figure 1.** (A) Zeta potential as a function of pH for various high-power/high-frequency materials. Zeta potentials of hydrogen and oxygen treated nanodiamonds (DND) are also plotted in the same graph.[5,29,39,40] The line at 0 mV was drawn for reference. (B) Atomic force micrograph of seeding with density approaching $10^{12}$ $cm^{-2}$. (C) Atomic force micrograph of seeding with density $\sim 10^{6}$ $cm^{-2}$. Reproduced with permission from ref 27. Copyright 2011 Elsevier.

Diamond (UDD).[24] Unfortunately, these 5 nm particles agglutinate into very large structures (>100 nm) which results in low nucleation densities. Efficient dispersion of these agglutinates took several decades from the initial discovery of the material but led to record breaking nucleation densities[25] and is now the most common approach to diamond seeding for thin films.

A critical difference between the earlier approaches with larger diamond particles and the dispersed 5 nm ones is their behavior in solution. Suspensions made with particles greater than one micron are prone to sedimentation due to gravity, whereas dispersed 5 nm solutions are true colloids with stability lasting several decades in water. This stability originates from the electrostatic repulsion of the particles from each other, a consequence of their net charge in solution or, more accurately "zeta potential". These charges originate from interactions between the surfaces of the diamond particles and the solvent. For example, diamond particles that have been annealed in air or purified in highly oxidizing solutions generally exhibit strong negative zeta potentials in water. This is because carboxyl (COOH) groups on the surface tend to become deprotonated, i.e., dissociate to $COO^{-}$ which is negatively charged while the solvent, water in the case becomes more acidic (dues to increased $H^{+}$). Of course, this dissociation is more prevalent at higher pH due to lower $H^{+}$ concentrations in the solvent; thus, zeta potentials are fundamentally pH dependent and should be quoted with the pH at which they were measured. A shorthand for this is the "isoelectric point", which is the pH at which the zeta potential is zero. At lower pH than the isoelectric point, the zeta potential will be positive, and at higher pH, negative. A secondary consequence of this proton donation is that colloids of acid treated/oxidized diamond nanoparticles have increasingly acidic pH with increasing particle concentration whereas the opposite if true for positively charge particles.[26]

An application of this zeta potential is that particles can be attracted to or repelled from surfaces depending on the associated charge of the surface, and this should be considered when trying to create dense layers of nanoparticles. This also explains why early attempts to use detonation nanodiamonds as seeds were unsuccessful, as the materials were acid cleaned and thus of a negative zeta potential. Silicon surfaces also exhibit a negative zeta potential across the majority of the pH range and thus the like charges repel one another in solution leading to low nucleation densities.[27] In fact, the first demonstration of high nucleation densities was somewhat fortunate in that the milling process used to separate the agglutinates generated a positive zeta potential,[28] which drove self-assembly of the nanoparticles to the silicon surface. There are now several methods for producing positive[29,26] or negative zeta potential[30,31] diamond nanoparticles, and thus, if the zeta potential of the substrate is known, it is just a case of choosing the particle with the opposite charge.

Figure 1 summarizes the zeta potentials as a function of pH for the substrates we have characterized to date, along with hydrogen and oxygen terminated nanodiamonds (DND) as the positive and negative seeds, respectively. It can be seen from this figure that the overwhelming majority of materials exhibit a negative zeta potential across the majority of the pH range (i.e., they have low isoelectric points, below pH 5) with the exception of the Ga face of GaN and $Al_2O_3$ deposited by Atomic Layer Deposition (ALD). In the case of GaN, the Ga-face and N-face exhibit differing zeta potential behavior as a function of pH. The


https://doi.org/10.1021/accountsmr.4c00126
Acc. Mater. Res. XXXX, XXX, XXX−XXX

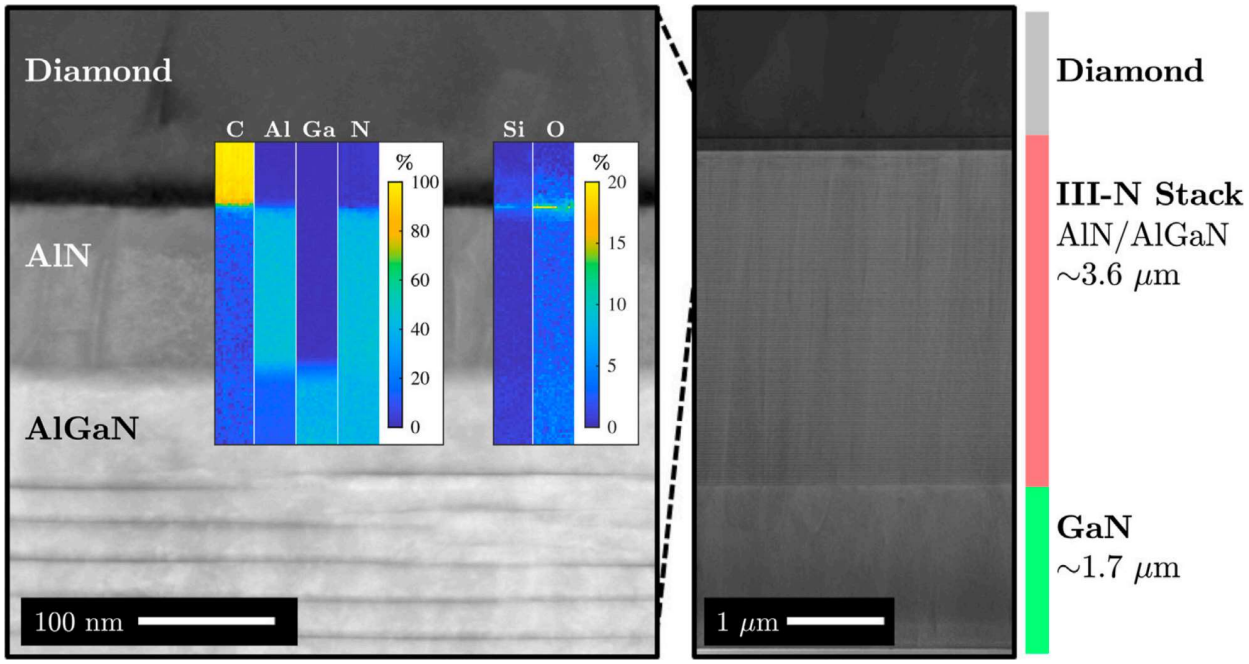


**Figure 2.** Cross-sectional HAADF-STEM micrograph and EDX data of CVD diamond grown on a 0.5 mm GaN/III−N membrane.[9] Reproduced with permission from ref 9. Copyright 2021 The Authors.

isoelectric point of the Ga-face is around pH 5.5, while that of the N-face is around pH 4. This difference is probably due to the higher oxygen adsorption ability of the N-face GaN,[32] the difference for seeding is however negligible. Sapphire and aluminum oxide grown by ALD also show small differences in isoelectric point (pH 4.5 vs pH 6 respectively) and are significantly different from aluminum oxide nanoparticles at pH 9.[33] Gallium oxide shows similar effects with bulk single crystal isoelectric point around 5 whereas the nanoparticles of the same can be up to pH 9.[34] Aluminum Nitride (AlN) is another highly complicated case, exhibiting both low (Figure 1, deposited by MOCVD) and high isoelectric points (nanoparticles)).[35]

AlN is complex due to the ease at which it oxidizes, and thus due to partial/complete oxidation, surfaces between different wafers can be drastically different. Thus, the structure of the material, as well as its surface termination, can influence the pH dependency of the zeta potential. Oxides such as $LiNbO_3$, $LiTaO_3$, $SiO_2$ (ALD), and quartz show much simpler behaviors, with low isoelectric points and little variation between wafers. The SiN surface exhibits a widely different isoelectric point after different cleaning steps. XPS studies revealed a direct correlation between low oxygen content on the surface and high iso electric point. While SC-1 cleaning was able to remove organic contaminants leading to low surface oxygen, oxygen plasma resulted in robustly oxygen terminated surfaces leading to quartzlike behavior. Full details of the cleaning procedure can be found in Bland et al.[36] From these results, it is clear that surface cleaning procedures have a profound effect on the surface termination/zeta potential and thus can influence the seeding of the substrates.

Figure 1B demonstrates the efficacy of this approach using opposite polarity zeta potentials for the substrate and seeds. In this case, the substrate is silicon and the seeds are hydrogen treated diamond nanoparticles. The final density is approaching the tip convolution limited resolution of the Atomic Force Microscope at $10^{12}$ $cm^{-2}$. If the substrate and seed have identical polarity zeta potentials, then the density is 6 orders of magnitude lower (Figure 1C). It should be noted that other approaches can be used to manipulate the zeta potential of substrates such as the use of polymers of opposite polarity[37] and plasma treatments.[38]

## 3. ADHESION AND SUBSTRATE EFFECTS

High densities of nuclei/seeds are a prerequisite for the growth of thin films of diamond on nondiamond substrates but are not sufficient. This is evident in cases such as GaN, $Ga_2O_3$, $LiNbO_3$, and $LaTaO_3$, where it is possible to generate very high seeding densities but after growth the films will delaminate on cooling to room temperature. This is due to a combination of effects, and each material needs to be considered independently; however, in the general case of seeding, clearly the diamond nanoparticles need to react with the substrate and form a stable carbide. The strength of this carbide bond needs to be able to withstand thermal stresses generated by the mismatch in thermal expansion coefficients. "High densities" are also very much within the eye of the beholder as the very abrupt interfaces generated by the highest density nanoseeding ($>10^{11}cm^{-2}$) generally result in poorer adhesion for applications such as tooling where densities around $<10^{10}$ $cm^{-2}$ provide a rougher and more mechanically robust interface. Many materials such as GaN, $Ga_2O_3$, $LiNbO_3$, $LaTaO_3$, etc. are also vulnerable to atomic hydrogen and in extreme cases will leach liquid gallium into the plasma.[5] The vapor pressure of substrates such as Fe, Co, Ni, Cr, etc. can also interfere with the initial stages of growth.[41]

A common approach to mitigating the above issues is to use an interlayer between the substrate and the diamond. SiN interlayers have been demonstrated to enable nucleation on GaN with great success, the result of which is now commercialized.[42] AlN or AlGaN is also a good option between GaN and diamond for enhancing adhesion, and it can be grown epitaxially on GaN.[9] Figure 2 shows an example of an AlN/


https://doi.org/10.1021/accountsmr.4c00126
Acc. Mater. Res. XXXX, XXX, XXX−XXX

**Table 2. Thermal Stress Mismatch Estimations with a Diamond**

| | Si | SiC | GaN | $Ga_2O_3$ | Diamond | Units | ref |
|---|---|---|---|---|---|---|---|
| Young's Modulus | 168 | 392 | 311 | 261 | 1000 | GPa | 9, 44−46 |
| Change in CTE$\alpha$(25 °C)- $\alpha$(800 °C) | −1.7 | −2.7 | −1.76 | −4.3 | −3.5 | ppm $K^{-1}$ | 43, 47 |
| Tensile Strength | 0.7 | >2 | >4 | >7 | >4 | GPa | 48−54 |
| Thin Film Stress on a Diamond Substrate[a] | 0.24 | 0.26 | 0.43 | −0.15 | - | GPa | |

[a]Temperature dependent CTE over a CVD range $\Delta T$ = 800−25 °C.

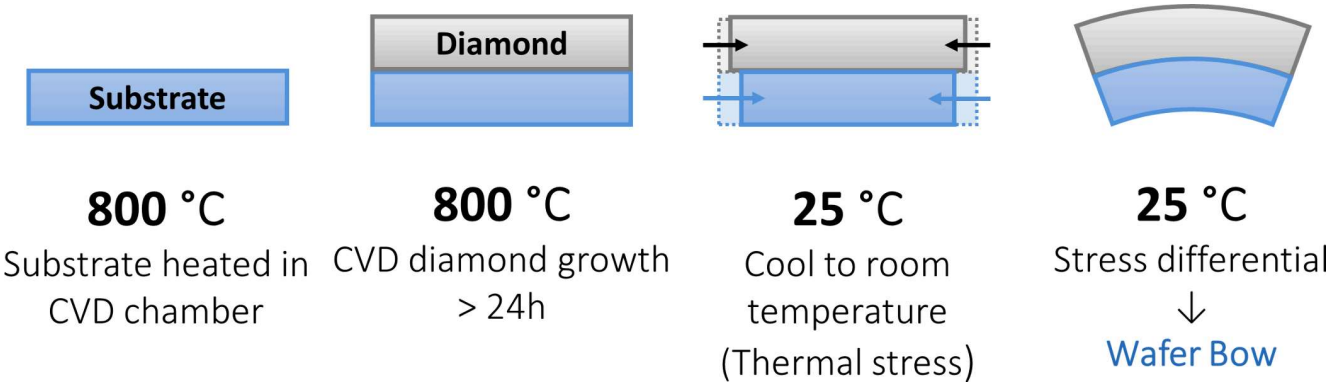


**Figure 3.** Diamond film on the substrate.

AlGaN stack between GaN and diamond membrane, exhibiting a highly abrupt interface and strong adhesion. This High-angle annular dark-field (HAADF) image from Scanning Transmission electron microscopy (STEM) shows a thick carbon rich (diamond) layer bound to an aluminum and nitrogen rich (AlN) layer. There is also a very thin layer of silicon and oxygen which originates from the silicon handle structure beneath the GaN.

## 4. THERMAL STRESS

One of the greatest challenges of direct heteroepitaxial growth of diamond using CVD on any semiconducting substrate is the high stresses incurred. Since CVD typically occurs at high temperatures, thermal stresses occur owing to the differing coefficients of thermal expansion (CTE) of diamond and the materials in the substrate. The materials are bound at the interface but have differing strain profiles upon cooling, resulting in either tensile or compressive stresses in the layer. In general, the thermal stress $\sigma$ in 1D is given by

$$\sigma(T) = E_{\text{layer}}\Delta T\Delta\alpha(T)$$

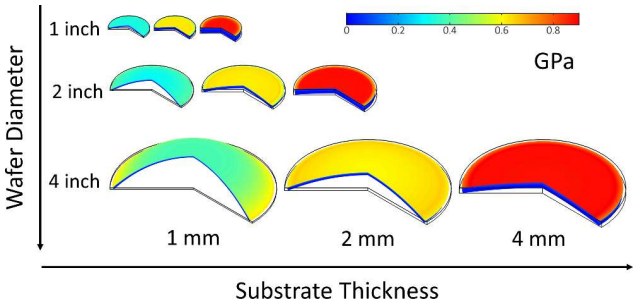


**Figure 4.** Axisymmetric finite element model of von Mises stresses with cross sections and exaggerated displacement fields (×50) of 100 $\mu$m diamond on Si cooled to room temperature from 800 °C using CTE data from,[43] deformation scale exaggerated by arbitrary value for visibility.

where $E_{\text{layer}}$ is Young's modulus, $T$ is the temperature, and $\alpha$ is the linear CTE. Large thermal stresses in the layers incur owing to a high Young's modulus, high diamond deposition temperatures (in excess of 800 °C), and diamond's low CTE compared to other materials.[43] As such, diamond in most cases is held in compression, while the other layers are in tension. This formula provides a general estimate of the interfacial stresses between the materials and whether the deposition will survive the CVD diamond process. Table 2 collates literature data and provides some general calculations of the thermal stress mismatch on diamond at ($\Delta T$ = 800−25 °C).

It is important to note that these simplified calculations assume that a thick layer of diamond is deposited onto a freestanding thin film. These results provide some insight into the magnitude of stress that the material will undergo during the CVD thermal cycling process. Since the materials have varying CTE's the difference in strain results in "wafer bow" as is shown in Figure 3. This is because the materials are bound at the interface in the 1D radial direction, and thus, the thermal stress can only be relieved through 2D out-of-plane wafer deformations. For cylindrical 2-layer systems, the magnitude of this bow is described by the Stoney formula through the radius of curvature and the biaxial modulus:[55]

$$R = E'\frac{t_{\text{sub}}^2}{t_{\text{film}}}\frac{1}{6}\frac{1}{\sigma_{\text{total}}}$$

where "sub" and "film" denote the substrate and film properties, respectively, $E' = \left[\frac{E}{1-\nu}\right]$ is the biaxial modulus, $\nu$ is the Poisson's ratio, $t$ denotes the thickness, and $\sigma_{\text{total}}$ denotes the total stress in the film. The central bow can then be estimated:[9]

$$w = R\left(1 - \cos\left[\frac{r_{\text{sub}}}{R}\right]\right)$$

where $r$ is the radius of the substrate. Larger wafers suffer from significant bowing, ultimately making any subsequent device processing difficult. Thus, to minimize the bow (maximize $R$) for


https://doi.org/10.1021/accountsmr.4c00126
Acc. Mater. Res. XXXX, XXX, XXX−XXX

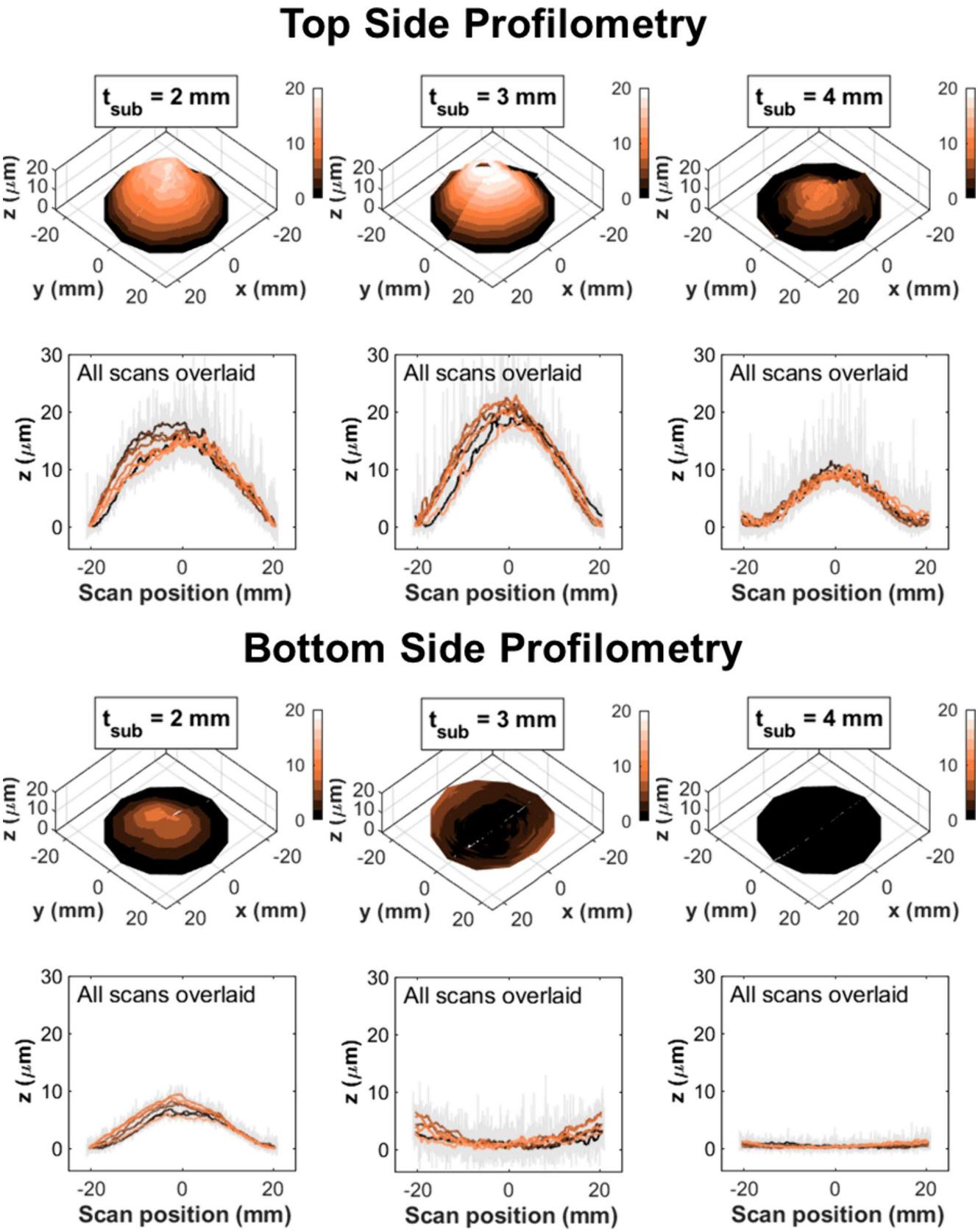


**Figure 5.** Surface profilometry of thick diamond films on 2" Si wafers of varying substrate thickness; top side radial profilometry data from ref 57 with additional bottom side data demonstrating reduced bow.



https://doi.org/10.1021/accountsmr.4c00126
*Acc. Mater. Res.* XXXX, XXX, XXX−XXX

larger wafers, it is clear that the substrate thickness of the substrate must be increased.

Here, one of the biggest challenges of diamond scalability is highlighted, where impractically thick substrates are the only way to sufficiently reduce the bow for high quality diamond growth on large wafers. Taking simple diamond on Si models from previous work has shown that even at 1 mm substrate thicknesses of silicon, the bow is still several hundred microns.[56] Going to much thicker substrates, a simple thermal stress finite element model of diamond on Si is shown in Figure 4. These simple modeling results clearly show the effect of substrate thickness and wafer diameter on the relative deformation and residual stresses, von Mises stress; also note that the computed von Mises residual stresses in FEM solutions are generally different to the simple 1D thermal stress model.[9] Although less practical for the large wafer scale, the substrate thickness effect was experimentally shown for 40−46 $\mu$m thick (by mass) diamond growth on 2 in. Si wafers as shown in Figure 5,[57] where the seemingly bowed top surface profilometry was actually a thickness variation since the Si underside was actually relatively flat in comparison. In this work, the authors demonstrate that both spatial variation and bow over 2 in. are best eliminated with 4 mm thick Si.

To reduce bowing and thermal stress as a whole, the growth temperature can be reduced; however, this results in lower quality diamond and much lower growth rates owing to the reduced H radical density at lower power and pressure.[58] Thus, assuming the materials can survive such stress, prestressing wafers in the opposite direction to counteract wafer bow is a potential solution for thin substrates.

## 5. CONCLUSION

The last two decades have seen substantial advances in the heterogeneous integration of diamond. The conditions that must be met for the successful growth of diamond on a nondiamond material are mostly known, however as we have tried to demonstrate above, they are multifaceted and often not all met in their entirety. For example, being able to nucleate and grow thin films of diamond on a material is not evidence of being able to grow the 10−100s of microns on it required for efficient thermal management. The anomalously low coefficient of thermal expansion of diamond creates real challenges as the growth temperature of diamond at commercially relevant growth rates is high (>700C). This is a mostly unavoidable physical constraint, and new approaches such as room temperature Surface Activated Wafer Bonding provide an exciting circumvention of this critical issue. Direct diamond growth on materials (or via an enabling interlayer) is still highly relevant for materials such as silicon, some III-Vs, metals, etc.; however, materials that do not form a stable carbide, have high thermal expansion coefficients, or are vulnerable to hydrogen plasmas are likely best served by wafer bonding approaches that can integrate the materials after their isolated growth processes.

## AUTHOR INFORMATION


### Corresponding Authors

**Oliver A. Williams** − *Cardiff School of Physics and Astronomy, Cardiff University, Cardiff CF24 3AA, United Kingdom;* orcid.org/0000-0002-7210-3004; Email: williamso@cardiff.ac.uk

**Soumen Mandal** − *Cardiff School of Physics and Astronomy, Cardiff University, Cardiff CF24 3AA, United Kingdom;* orcid.org/0000-0001-8912-1439; Email: MandalS2@cardiff.ac.uk

**Jerome A. Cuenca** − *Cardiff School of Physics and Astronomy, Cardiff University, Cardiff CF24 3AA, United Kingdom;* orcid.org/0000-0003-1370-1167; Email: cuencaj@cardiff.ac.uk

Complete contact information is available at: https://pubs.acs.org/10.1021/accountsmr.4c00126


### Author Contributions

‡O.A.W., S.M., and J.A.C. contributed equally to this paper.

### Notes

The authors declare no competing financial interest.

### Biographies

**Oliver A. Williams** received his BEng in 1998 and PhD in 2003, both from University College London. He then worked as a Center for Nanoscale Materials Distinguished Postdoc in the Nanocarbon theme at Argonne National Laboratory between 2003/4. Following this he moved to IMO/IMEC in Hasselt University Belgium where he worked as a Research Scientist for four years. He then accepted an "Attract" award at the Fraunhofer Institute for Applied Solid State Research in Freiburg, Germany where he was team leader of Diamond Technology for three years. He is now a Professor in Experimental Physics at Cardiff School of Physics and Astronomy. His research group, Cardiff Diamond Foundry, focuses on diamond growth and technology towards SAW, MEMS, Thermal Management, nanoparticles, superconductivity and quantum technologies.

**Soumen Mandal** completed his PhD in experimental condensed matter physics as part of the MSc-PhD Dual Degree program at the Indian Institute of Technology Kanpur in 2009. Following his doctoral studies, he undertook a postdoctoral research position at Institut Neel in Grenoble, France. In 2013, he joined Cardiff University in the United Kingdom as a Research Associate. Dr. Mandal's research focuses on spintronics, thin magnetic films, superconductor-ferromagnet multilayers, superconducting diamond devices, diamond thin film growth, and diamond nanoparticles. Currently, his research interests include diamond-based devices, diamond thin film nucleation and growth, and diamond nanoparticles.

**Jerome A.Cuenca** completed his PhD in microwave engineering and materials science at the Centre for High Frequency Engineering at Cardiff University in 2015. He joined the Cardiff Diamond Foundry as a Research Associate in 2017. His primary research focuses are on microwave dielectric spectroscopy systems for carbonaceous materials, microwave applications of diamond, microwave plasma chemical vapour deposition of diamond and the optimization of plasma reactors using finite element modelling.

## REFERENCES


(1) Gajewski, W.; Achatz, P.; Williams, O. A.; Haenen, K.; Bustarret, E.; Stutzmann, M.; Garrido, J. A. Electronic and Optical Properties of Boron-Doped Nanocrystalline Diamond Films. *Phys. Rev. B* **2009**, *79* (4), No. 045206.

(2) Koizumi, S.; Teraji, T.; Kanda, H. Phosphorus-Doped Chemical Vapor Deposition of Diamond. *Diam. Relat. Mater.* **2000**, *9* (3−6), 935−940.

(3) Balasubramanian, G.; Neumann, P.; Twitchen, D.; Markham, M.; Kolesov, R.; Mizuochi, N.; Isoya, J.; Achard, J.; Beck, J.; Tissler, J.; Jacques, V.; Hemmer, P. R.; Jelezko, F.; Wrachtrup, J. Ultralong Spin Coherence Time in Isotopically Engineered Diamond. *Nat. Mater.* **2009**, *8* (5), 383−387.

(4) Li, S.; Li, S.; Zheng, Q.; Lv, Y.; Liu, X.; Wang, X.; Huang, P. Y.; David, G.; Lv, B. High Thermal Conductivity in Cubic Boron Arsenide Crystals. *Science (80-.)* **2018**, *361*, 579.
(5) Mandal, S.; Arts, K.; Knoops, H. C. M.; Cuenca, J. A.; Klemencic, G. M.; Williams, O. A. Surface Zeta Potential and Diamond Growth on Gallium Oxide Single Crystal. *Carbon* **2021**, *181*, 79−86.
(6) Mandal, S.; Thomas, E. L. H.; Middleton, C.; Gines, L.; Griffiths, J. T.; Kappers, M. J.; Oliver, R. A.; Wallis, D. J.; Goff, L. E.; Lynch, S. A.; Kuball, M.; Williams, O. A. Surface Zeta Potential and Diamond Seeding on Gallium Nitride Films. *ACS Omega* **2017**, *2* (10), 7275−7280.
(7) Wang, J.; Butler, J. E.; Feygelson, T.; Nguyen, C. T. C. 1.51-GHz Nanocrystalline Diamond Micromechanical Disk Resonator with Material-Mismatched Isolating Support. In *Mems 2004:17th Ieee International Conference on Micro Electro Mechanical Systems, Technical Digest*; Proceedings IEEE Micro Electro Mechanical Systems Workshop; 2004; pp 641−644.
(8) Rodriguez-Madrid, J. G.; Iriarte, G. F.; Pedros, J.; Williams, O. A.; Brink, D.; Calle, F. Super-High-Frequency SAW Resonators on AlN/Diamond. *IEEE Electron Device Lett.* **2012**, *33* (4), 495−497.
(9) Cuenca, J. A.; Smith, M. D.; Field, D. E.; Massabuau, F. C.-P.; Mandal, S.; Pomeroy, J.; Wallis, D. J.; Oliver, R. A.; Thayne, I.; Kuball, M.; Williams, O. A. Thermal Stress Modelling of Diamond on GaN/III-Nitride Membranes. *Carbon* **2021**, *174*, 647−661.
(10) Daenen, M.; Williams, O. A.; D'Haen, J.; Haenen, K.; Nesládek, M. Seeding, Growth and Characterization of Nanocrystalline Diamond Films on Various Substrates. *Phys. status solidi* **2006**, *203* (12), 3005−3010.
(11) Rodríguez-Madrid, J. G.; Iriaróte, G. F.; Pedros, J.; Williams, O. A.; Brink, D.; Calle, F. Super-High-Frequency SAW Resonators on AlN/Diamond. *IEEE Electron Device Lett.* **2012**, *33* (4), 495−497.
(12) Gerrer, T.; Cimalla, V.; Waltereit, P.; Müller, S.; Benkhelifa, F.; Maier, T.; Czap, H.; Ambacher, O.; Quay, R. Transfer of AlGaN/GaN RF-Devices onto Diamond Substrates via van Der Waals Bonding. *Int. J. Microwave Wireless Technol.* **2018**, *10* (5−6), 666−673.
(13) Rabarot, M.; Widiez, J.; Saada, S.; Mazellier, J. P.; Lecouvey, C.; Roussin, J. C.; Dechamp, J.; Bergonzo, P.; Andrieu, F.; Faynot, O.; et al. Silicon-On-Diamond Layer Integration by Wafer Bonding Technology. *Diam. Relat. Mater.* **2010**, *19* (7−9), 796−805.
(14) Ren, Z.; Xu, J.; Le, X.; Lee, C. Heterogeneous Wafer Bonding Technology and Thin-Film Transfer Technology-Enabling Platform for the next Generation Applications beyond 5g. *Micromachines* **2021**, *12* (8), 946.
(15) Matsumae, T.; Kurashima, Y.; Umezawa, H.; Takagi, H. Hydrophilic Low-Temperature Direct Bonding of Diamond and Si Substrates under Atmospheric Conditions. *Scr. Mater.* **2020**, *175*, 24−28.
(16) Takagi, H.; Maeda, R.; Chung, T. R.; Suga, T. Low-Temperature Direct Bonding of Silicon and Silicon Dioxide by the Surface Activation Method. *Sensors Actuators, A Phys.* **1998**, *70* (1−2), 164−170.
(17) Waller, W. M.; Pomeroy, J. W.; Field, D.; Smith, E. J. W.; May, P. W.; Kuball, M. Thermal Boundary Resistance of Direct van Der Waals Bonded GaN-on-Diamond. *Semicond. Sci. Technol.* **2020**, *35*, No. 095021.
(18) Thomas, E. L. H.; Nelson, G. W.; Mandal, S.; Foord, J. S.; Williams, O. A. Chemical Mechanical Polishing of Thin Film Diamond. *Carbon* **2014**, *68*, 473−479.
(19) Thomas, E. L. H.; Mandal, S.; Brousseau, E. B.; Williams, O. A. Silica Based Polishing of {100} and {111} Single Crystal Diamond. *Sci. Technol. Adv. Mater.* **2014**, *15* (3), 035013.
(20) Liang, J.; Masuya, S.; Kim, S.; Oishi, T.; Kasu, M.; Shigekawa, N. Stability of Diamond/Si Bonding Interface during Device Fabrication Process. *Appl. Phys. Express* **2019**, *12* (1), 016501.
(21) Mandal, S. Nucleation of Diamond Films on Heterogeneous Substrates: A Review. *RSC Adv.* **2021**, *11* (17), 10159−10182.
(22) Iijima, S.; Aikawa, Y.; Baba, K. Early Formation of Chemical Vapor Deposition Diamond Films. *Appl. Phys. Lett.* **1990**, *57* (25), 2646−2648.
(23) Mandal, S.; Thomas, E. L. H.; Jenny, T. A.; Williams, O. A. Chemical Nucleation of Diamond Films. *ACS Appl. Mater. Interfaces* **2016**, *8* (39), 26220−26225.
(24) Danilenko, V. V. On the History of the Discovery of Nanodiamond Synthesis. *Phys. Solid State* **2004**, *46* (4), 595−599.
(25) Williams, O. A.; Douhéret, O.; Daenen, M.; Haenen, K.; Ōsawa, E.; Takahashi, M. Enhanced Diamond Nucleation on Monodispersed Nanocrystalline Diamond. *Chem. Phys. Lett.* **2007**, *445* (4−6), 255−258.
(26) Ginés, L.; Mandal, S.; Ashek-I-Ahmed, A.-I.-A.; Cheng, C.-L.; Sow, M.; Williams, O. A. Positive Zeta Potential of Nanodiamonds. *Nanoscale* **2017**, *9* (34), 12549−12555.
(27) Hees, J.; Kriele, A.; Williams, O. A. Electrostatic Self-Assembly of Diamond Nanoparticles. *Chem. Phys. Lett.* **2011**, *509*, 12.
(28) Ozawa, M.; Inaguma, M.; Takahashi, M.; Kataoka, F.; Krüger, A.; Osawa, E. Preparation and Behavior of Brownish, Clear Nanodiamond Colloids. *Adv. Mater.* **2007**, *19* (9), 1201−1206.
(29) Williams, O. A.; Hees, J.; Dieker, C.; Jäger, W.; Kirste, L.; Nebel, C. E. Size-Dependent Reactivity of Diamond Nanoparticles. *ACS Nano* **2010**, *4* (8), 4824−4830.
(30) Osswald, S.; Yushin, G.; Mochalin, V.; Kucheyev, S. O.; Gogotsi, Y. Control of Sp2/Sp3 Carbon Ratio and Surface Chemistry of Nanodiamond Powders by Selective Oxidation in Air. *J. Am. Chem. Soc.* **2006**, *128* (35), 11635−11642.
(31) Stehlik, S.; Varga, M.; Ledinsky, M.; Miliaieva, D.; Kozak, H.; Skakalova, V.; Mangler, C.; Pennycook, T. J.; Meyer, J. C.; Kromka, A.; Rezek, B. High-Yield Fabrication and Properties of 1.4 Nm Nanodiamonds with Narrow Size Distribution. *Sci. Rep.* **2016**, *6* (December), 1−8.
(32) Zywietz, T. K.; Neugebauer, J.; Scheffler, M. The Adsorption of Oxygen at GaN Surfaces. *Appl. Phys. Lett.* **1999**, *74* (12), 1695−1697.
(33) Bahena, J. L. R.; Cabrera, A. R.; Valdivieso, A. L.; Urbina, R. H. Fluoride Adsorption onto $\alpha$-Al2O3 and Its Effect on the Zeta Potential at the Alumina-Aqueous Electrolyte Interface. *Sep. Sci. Technol.* **2002**, *37* (8), 1973−1987.
(34) Kosmulski, M. Pristine Points of Zero Charge of Gallium and Indium Oxides. *J. Colloid Interface Sci.* **2001**, *238* (1), 225−227.
(35) Hees, J.; Heidrich, N.; Pletschen, W.; Sah, R. E.; Wolfer, M.; Williams, O. A.; Lebedev, V.; Nebel, C. E.; Ambacher, O. Piezoelectric Actuated Micro-Resonators Based on the Growth of Diamond on Aluminum Nitride Thin Films. *Nanotechnology* **2013**, *24* (2), No. 025601.
(36) Bland, H. A.; Thomas, E. L. H.; Klemencic, G. M.; Mandal, S.; Morgan, D. J.; Papageorgiou, A.; Jones, T. G.; Williams, O. A. Superconducting Diamond on Silicon Nitride for Device Applications. *Sci. Rep.* **2019**, *9*, 2911.
(37) Girard, H. A.; Perruchas, S.; Gesset, C.; Chaigneau, M.; Vieille, L.; Arnault, J. C.; Bergonzo, P.; Boilot, J. P.; Gacoin, T. Electrostatic Grafting of Diamond Nanoparticles: A Versatile Route to Nanocrystalline Diamond Thin Films. *ACS Appl. Mater. Interfaces* **2009**, *1* (12), 2738−2746.
(38) Pobedinskas, P.; Degutis, G.; Dexters, W.; Janssen, W.; Janssens, S. D.; Conings, B.; Ruttens, B.; D'Haen, J.; Boyen, H. G.; Hardy, A.; Van Bael, M. K.; Haenen, K. Surface Plasma Pretreatment for Enhanced Diamond Nucleation on AlN. *Appl. Phys. Lett.* **2013**, *102* (20), 1−5.
(39) Mandal, S.; Yuan, C.; Massabuau, F.; Pomeroy, J. W.; Cuenca, J.; Bland, H.; Thomas, E.; Wallis, D.; Batten, T.; Morgan, D.; Oliver, R.; Kuball, M.; Williams, O. A. Thick, Adherent Diamond Films on AlN with Low Thermal Barrier Resistance. *ACS Appl. Mater. Interfaces* **2019**, *11* (43), 40826−40834.
(40) Mandal, S.; Arts, K.; Morgan, D. J.; Chen, Z.; Williams, O. A. Zeta Potential and Nanodiamond Self Assembly Assisted Diamond Growth on Lithium Niobate and Lithium Tantalate Single Crystal. *Carbon* **2023**, *212* (May), No. 118160.
(41) Lux, B.; Haubner, R. Diamond Substrate Interactions and the Adhesion of Diamond Coatings. *Pure Appl. Chem.* **1994**, *66* (9), 1783−1788.


https://doi.org/10.1021/accountsmr.4c00126
*Acc. Mater. Res.* XXXX, XXX, XXX−XXX

(42) Francis, D.; Faili, F.; Babić, D.; Ejeckam, F.; Nurmikko, A.; Maris, H. Formation and Characterization of 4-Inch GaN-on-Diamond Substrates. *Diam. Relat. Mater.* **2010**, *19* (2−3), 229−233.
(43) Slack, G. A.; Bartram, S. F. Thermal Expansion of Some Diamondlike Crystals. *J. Appl. Phys.* **1975**, *46* (1), 89−98.
(44) Zheng, X. Q.; Zhao, H.; Jia, Z.; Tao, X.; Feng, P. X. L. Young's Modulus and Corresponding Orientation in $\beta$-Ga2O3 Thin Films Resolved by Nanomechanical Resonators. *Appl. Phys. Lett.* **2021**, *119* (1), No. 013505.
(45) Polian, A.; Grimsditch, M.; Grzegory, I. Elastic Constants of Gallium Nitride. *J. Appl. Phys.* **1996**, *79* (6), 3343−3344.
(46) Harris, G. L. *Properties of Silicon Carbide*, 13th ed.; IET, 1995.
(47) Cheng, Z.; Hanke, M.; Galazka, Z.; Trampert, A. Thermal Expansion of Single-Crystalline $\beta$ -Ga2O3 from RT to 1200 K Studied by Synchrotron-Based High Resolution x-Ray Diffraction. *Appl. Phys. Lett.* **2018**, *113* (18), 1−5.
(48) Greek, S.; Ericson, F.; Johansson, S.; Schweitz, J. Å. In Situ Tensile Strength Measurement and Weibull Analysis of Thick Film and Thin Film Micromachined Polysilicon Structures. *Thin Solid Films* **1997**, *292* (1−2), 247−254.
(49) Guo, W.; Gao, Y.; Hu, W.; Wu, X.; Zhou, H. Study on the Mechanical Property of High-Performance Silicon Carbide Fiber. *Adv. Eng. Mater.* **2022**, *24* (7), 1−7.
(50) Brown, J. J.; Baca, A. I.; Bertness, K. A.; Dikin, D. A.; Ruoff, R. S.; Bright, V. M. Tensile Measurement of Single Crystal Gallium Nitride Nanowires on MEMS Test Stages. *Sensors Actuators A Phys.* **2011**, *166* (2), 177−186.
(51) Yonenaga, I. Hardness, Yield Strength, and Dislocation Velocity in Elemental and Compound Semiconductors. *Mater. Trans.* **2005**, *46* (9), 1979−1985.
(52) Grashchenko, A. S.; Kukushkin, S. A.; Nikolaev, V. I.; Osipov, A. V.; Osipova, E. V.; Soshnikov, I. P. Study of the Anisotropic Elastoplastic Properties of $\beta$-Ga2O3 Films Synthesized on SiC/Si Substrates. *Phys. Solid State* **2018**, *60* (5), 852−857.
(53) Espinosa, H. D.; Peng, B.; Moldovan, N.; Friedmann, T. A.; Xiao, X.; Mancini, D. C.; Auciello, O.; Carlisle, J.; Zorman, C. A.; Merhegany, M. Elasticity, Strength, and Toughness of Single Crystal Silicon Carbide, Ultrananocrystalline Diamond, and Hydrogen-Free Tetrahedral Amorphous Carbon. *Appl. Phys. Lett.* **2006**, *89* (7), 1−4.
(54) Wu, Y. Q.; Gao, S.; Kang, R. K.; Huang, H. Deformation Patterns and Fracture Stress of Beta-Phase Gallium Oxide Single Crystal Obtained Using Compression of Micro-Pillars. *J. Mater. Sci.* **2019**, *54* (3), 1958−1966.
(55) Windischmann, H.; Epps, G. F.; Cong, Y.; Collins, R. W. Intrinsic Stress in Diamond Films Prepared by Microwave Plasma Cvd. *J. Appl. Phys.* **1991**, *69* (4), 2231−2237.
(56) Edwards, M. J.; Bowen, C. R.; Allsopp, D. W. E.; Dent, A. C. E. Modelling Wafer Bow in Silicon−Polycrystalline CVD Diamond Substrates for GaN-Based Devices. *J. Phys. D. Appl. Phys.* **2010**, *43* (38), No. 385502.
(57) Cuenca, J. A.; Leigh, W.; Thomas, E. L. H.; Mandal, S.; Williams, O. A. Modelling Deposition Uniformity in Microwave Plasma CVD Diamond over 2" Si Wafers. *IEEE* **2022**, 656−658.
(58) Cuenca, J. A.; Mandal, S.; Thomas, E. L. H.; Williams, O. A. Microwave Plasma Modelling in Clamshell Chemical Vapour Deposition Diamond Reactors. *Diam. Relat. Mater.* **2022**, *124* (February), No. 108917.


https://doi.org/10.1021/accountsmr.4c00126
*Acc. Mater. Res.* XXXX, XXX, XXX−XXX